Convective Heat Transfer Steady Heat Conduction and Thermal Stress in a Ceramic/FGM/Metal Composite EFBF Plate

Xu Yangjian
School of Civil Engineering, Hebei University of Engineering, Handan 056038, China
Email: xuyangjian@sohu.com

Tu Daihui
School of Science, Hebei University of Engineering, Handan 056038, China
Email: tdhui563@sina.com

Du Haiyang
School of Civil Engineering, Hebei University of Engineering, Handan 056038, China
Email: guduxing@126.com

***Abstract*—A finite element model is constructed to analyze the steady heat conduction and thermal stress in a ceramic/FGM/metal composite EFBF plate under convective heat transfer boundary. From numerical calculation, when $\bar{\zeta}_a = \bar{\zeta}_b = 1$, T_0=T_a =300K and T_b=1 800K, the steady heat conduction and thermal stress distributions in the plate were obtained. The numerical results show that the temperature distribution in the composite plate is more reasonable with the increase of the FGM layer thickness, and compared with h_2=2mm the maximum tensile stress of h_2=6mm reduces by 36.3%. With the increase of M, the temperature on the surface of ceramics reduces by 6.2%, the compressive stress on the metal surface reduces by 28.3%, and the compressive stress on the surface of ceramics increases by 70.2%. With the increase of porosity, there is an abrupt change for temperature at the $\bar{y}$≈0.48, its value is 875 K, and the change of stress at the interface of the three-layered plate increases, and the tensile stress on the surface of ceramics reaches the maximum. Compared with $\bar{\zeta}_a = \bar{\zeta}_b = 1$ when $\bar{\zeta}_a = \bar{\zeta}_b = 10$, the temperature on the surface of metal reduces by 23.9% and the temperature on the surface of ceramics increases by 44.4%, and the stress on the metal surface increases by 148% and the stress on the ceramic surface increases by 165%. Compared with the nongraded two-layered composite plate, the temperature and the thermal stress of the ceramic/FGM/metal composite plate are very gentle and smooth. The results provide the foundations of theoretical calculation for the design and application of the composite plate.**

***Index Terms*—ceramic/FGM/metal composite plate, steady heat conduction and thermal stresses, FEM, convective heat transfer boundary, EFBF mechanical boundary**

Address correspondence to Professor Xu Yangjian, School of Civil Engineering, Hebei University of Engineering, Handan 056038, China. Tel.: +86-0310-8578239

I. INTRODUCTION

Functionally graded material (FGM) is a new type of inhomogeneous composite material with special bonding characteristics duo to arbitrarily distributed and continuously varied material properties. The advantages of FGM are that such materials can reduce the magnitude of the residual and thermal stresses and increase the strength and fracture toughness. Therefore, FGMs have received considerable attention in the field of structural design subjected to extremely high thermal loading [1-8]. Because it is used widely in high temperature working environment such as aviation and nuclear reactor, and so on, it is important to analyze the thermal stress filed of the body made of the material.

Obata [9-10] and Tanigawa [11] researched thermal stress of pure FGM plate by adopting perturbation and laminated analytical method, respectively. Huang [12] analyzed the thermal elastic limitation of four-layered composite plate with FGM in the middle of the plate. But these methods are too complex so as to lead to a complicated equation system, and are not convenient for engineering application. Therefore, Xu [13-14] studied the problem of transient thermal stress of pure FGM plate under convective heat transfer boundary and during heating and cooling process by adopting simple NFEM.

Based on the above research work, without loss of generality, we present a model of analysis that is ceramic/FGM/metal composite plate. The new composite plate has the advantages of FGM and composite plate. Such as, the heat-resistant and mechanical properties of the new composite plate are better than those of pure FGM plate, and under the same thickness of plate the fabrication cost of the new composite plate is lower than that of pure FGM plate.

© 2011 ACADEMY PUBLISHER
doi:10.4304/jsw.6.2.201-208

In the present article, starting from the heat conduction law, this paper will discuss the steady thermal stress problem of a ZrO_2/FGM/Ti-6Al-4V composite EFBF plate under convective heat transfer boundary by the FEM and the Sinpson method. We hope that the analytical results obtained will be more close to actual engineering conditions and to obtain some instructive conclusions for the production and application of ceramic/FGM/metal composite plate.

II. Model of Analysis

As shown in Fig. 1, we now consider the steady thermal stress field distributions of a three-layered infinitely long composite EFBF plate made of metal (Ti-6Al-4V) and ceramics (ZrO_2) with an interlayer of FGM under convective heat transfer boundary. We have the following assumptions. (1) The lower layer of three-layered plate is metal; k_m, E_m, α_m and υ_m denote thermal conductivity, Young's modulus, the coefficient of linear thermal expansion and Poisson's ratio of the metal layer, respectively, and the layer thickness is h_1. The middle is continuous and arbitrary variant FGM gradient layer; $k(y)$, $E(y)$, $\alpha(y)$ and $\upsilon(y)$ denote the above material properties of FGM gradient layer, and the layer thickness is $h_2=h_{FGM}$. The upper layer is ceramics; k_c, E_c, α_c and υ_c denote the above material properties of ceramic layer, and the layer thickness is h_3. (2) Initially, the plate is under the stress-free status; the initial temperature of the plate is T_0; the plate is heated from the lower and upper surfaces by surrounding media with heat transfer coefficients ζ_a and ζ_b, respectively, and we denote the temperature of the surrounding media by constant T_a and T_b. (3) The periphery of the plate is adiabatic, and there are no heat sources within the plate. Coordinate axis y is chosen as shown in Fig. 1, and the interfaces between the layers are perfectly bonded at all times. T is temperature function. The material's properties for each same ordinate y are homogeneous and isotropic. Subscripts c and m mean ceramics and metal, respectively. The total thickness of the plate is $b = h_1+h_2+h_3$ and $b_1 = h_1$, $b_2 = h_1+h_2$.

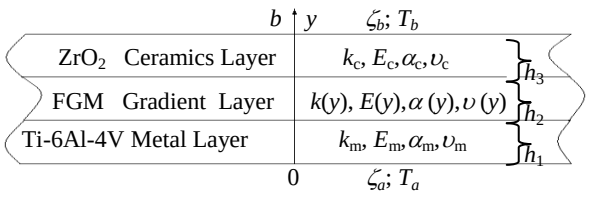

Figure 1. Ceramic/FGM/metal composite plate.

III. Heat Conduction Analysis

The steady thermal conduction basic equation of the i th layer of the three-layered composite plate is

$$0 = \frac{d}{dy}\left\{k_i(y)\frac{dT_i(y)}{dy}\right\}, i = 1,2,3, \tag{1}$$

where $k_i(y)$ is the thermal conductivity of per layer of the three-layered composite plate (such as i =1, $k_1(y)$ = k_m, the rest on the analogy of this). Thermal conductivity of the FGM layer is $k(y)$. The convective heat transfer boundary and the conditions of continuity of the temperature in the three-layered composite plate and the heat flux at interfaces are expressed in the following form

$$\left.\begin{aligned} y = 0, k_m\frac{dT_1(y)}{dy} - \zeta_a T_1(y) = -\zeta_a T_a \\ y = b, k_c\frac{dT_3(y)}{dy} + \zeta_b T_3(y) = \zeta_b T_b \end{aligned}\right\}, \tag{2}$$

$$\left.\begin{aligned} y_i = b_i,\ T_i(y_i) = T_{i+1}(y_i), \quad i = 1,2 \\ k_i(y_i)\frac{dT_i(y_i)}{dy} = k_{i+1}(y_i)\frac{dT_{i+1}(y_i)}{dy} \end{aligned}\right\}. \tag{3}$$

When solving the steady heat conduction problem of linear control equations approximately by adopting FEM, we need to establish relevant functional. The paper adopts one-dimensional FEM to solve the above problem. Under the condition of assumption in this paper, the element functional [15] (5.14) of one-dimensional steady heat conduction problem under the convective heat transfer boundary condition is

$$\pi_e = \int_e \frac{k^e}{2}\left(\frac{dT}{dy}\right)^2 dy + \zeta^e\left(\frac{T^2}{2} - \hat{T}_\Gamma T\right), \tag{4}$$

where ζ^e, k^e are convective heat transfer coefficient and the thermal conductivity of the element, respectively, the constant values, and not the function of y, but these values are different for different element. $\hat{T}_\Gamma$ is the environmental media temperature, and Γ is the boundary of given convective heat transfer condition.

Consider bar element, the element length is l^e, and two nodes are denoted by i, j. The trial function of temperature field is linear distribution.

$$T = a_1 + a_2 y, \tag{5}$$

where a_1, a_2 are the unknown constants.

The temperature of node r is denoted by Tr (r = i, j), we have

$$T_r = a_1 + a_2 y_r, \quad r = i, j. \tag{6}$$

We have for any element

$$T_i = a_1 + a_2 y_i, \quad T_j = a_1 + a_2 y_j. \tag{7}$$

Then we can write Eq. (7) in matrix form

$$\begin{bmatrix} 1 & y_i \\ 1 & y_j \end{bmatrix}\begin{Bmatrix} a_1 \\ a_2 \end{Bmatrix} = \begin{Bmatrix} T_i \\ T_j \end{Bmatrix}. \tag{8}$$

The unknown constants a_1, a_2 in the Eq. (8) can be solved by using of the method of matrix inverse.

$$\begin{Bmatrix} a_1 \\ a_2 \end{Bmatrix} = \begin{bmatrix} 1 & y_i \\ 1 & y_j \end{bmatrix}^{-1}\begin{Bmatrix} T_i \\ T_j \end{Bmatrix} = \frac{1}{y_j - y_i}\begin{bmatrix} 1 & -y_i \\ 1 & y_j \end{bmatrix}\begin{Bmatrix} T_i \\ T_j \end{Bmatrix}. \tag{9}$$

Hence

© 2011 ACADEMY PUBLISHER

$$a_1 = \frac{1}{y_j - y_i}\left(y_j T_i - y_i T_j\right),\ a_2 = \frac{1}{y_j - y_i}\left(-T_i + T_j\right). \quad (10)$$

Substitution of Eq. (10) into Eq. (5) yields the trial function of temperature field:

$$T = \frac{y_j - y}{l^e} T_i + \frac{y - y_i}{l^e} T_j \ . \quad (11)$$

Then we can write Eq. (11) in matrix form

$$T = N_i T_i + N_j T_j = \begin{pmatrix} N_i & N_j \end{pmatrix} \begin{pmatrix} T_i \\ T_j \end{pmatrix} = N T^e \ , \quad (12)$$

where

$$N = \begin{pmatrix} N_i & N_j \end{pmatrix}, N_i = \frac{y_j - y}{l^e}, N_j = \frac{y - y_i}{l^e}, T^e = \begin{pmatrix} T_i \\ T_j \end{pmatrix}. \quad (13)$$

The T in Eq. (12) is the any point temperature on element e. The ordinate y of the nodes i, j in element e can be written by y_i, y_j. We have

$$\text{Node } j: N_i = 0, N_j = 1, \text{ Node } i: \ N_i = 1, N_j = 0. \quad (14)$$

We can obtain by solving the first derivative of the trial function T of temperature field in Eq.(11) with respect to y

$$\frac{dT}{dy} = -\frac{1}{l^e} T_i + \frac{1}{l^e} T_j \ . \quad (15)$$

Substitution of Eq. (15) into Eq. (4) yields the functional of element e:

$$\pi_e = \frac{k}{2l^e}\left(T_i^2 - 2T_i T_j + T_j^2\right) + \frac{\zeta}{2}\left(T_j^{\ 2} - \hat{T}_\Gamma T_j\right). \quad (16)$$

Then we can write Eq. (16) in matrix form:

$$\pi_e = T_e^T \left(\frac{1}{2} h_e T_e - q_e\right), \quad (17)$$

where

$$q^e = \begin{bmatrix} q_i^e & q_j^e \end{bmatrix}^T = \begin{bmatrix} 0 & \frac{\zeta}{2}\hat{T}_\Gamma \end{bmatrix}^T, \quad (18)$$

$$h^e = \begin{bmatrix} h_{ii}^e & h_{ij}^e \\ h_{ji}^e & h_{jj}^e \end{bmatrix} = \frac{k^e}{l^e}\begin{bmatrix} 1 & -1 \\ -1 & 1 \end{bmatrix} + \zeta \begin{bmatrix} 0 & 1 \end{bmatrix}. \quad (19)$$

Under the convective heat transfer boundary condition, the finite element basic equation of steady heat conduction in the three-layered composite plate is (see [15] (5.26))

$$H\,T = Q, \quad (20)$$

where H, T and Q denote thermal stiffness matrix, unknown node temperature array and node thermal load array, respectively. The elements h_{rs}^e and q_r^e (r, s =i, j) in matrix H and Q are respectively

$$h_{rs}^e = \frac{k_{n-1}^e}{l^e}\left(2\delta_{rs} - 1\right) + \zeta_{n-1}^e \delta_{rj}, q_r^e = \frac{\zeta_{n-1}^e}{2}\hat{T}_\Gamma \delta_{rj}, \quad (21)$$

where δ_{rs} is the symbol of Kronecker δ.

IV. Thermal Stress Analysis

The strain components ε_{xxi}, ε_{zzi} and stress components σ_{xxi}, σ_{zzi} of the ith layer of the three-layered composite plate are given respectively by the relations [11]

$$\left.\begin{aligned} \varepsilon_{xxi}(\bar{y}) = \varepsilon_{zzi}(\bar{y}) &= \varepsilon_0 + \bar{y}/\bar{r}_0 \qquad (i = 1,2,3) \\ \sigma_{xxi}(\bar{y}) = \sigma_{zzi}(\bar{y}) &= \frac{E_i(\bar{y})}{1-\upsilon_i(\bar{y})} \times \left[\varepsilon_0 + \frac{\bar{y}}{\bar{r}_0} - \alpha_i(\bar{y}) T'(\bar{y})\right] \end{aligned}\right\}, \quad (22)$$

where $\bar{y} = y / b$ is dimensionless position coordinate, ε_0 and $1 / \bar{r}_0 = b / r$ denote strain component and dimensionless curvature on the $\bar{y} = 0$ plane respectively, $T'(\bar{y})$ is temperature rise, ε_0 and $1 / \bar{r}_0$ are unknown constants and they are determined by the mechanical boundary condition. Supposing that the plate can elongate and bend freely (EFBF), and the unknown constants are determined by the following equilibrium equations

$$\sum_i \int_{\bar{y}_{i-1}}^{\bar{y}_i} \sigma_{xxi}(\bar{y}) \bar{y} d\bar{y} = 0, \sum_i \int_{\bar{y}_{i-1}}^{\bar{y}_i} \sigma_{xxi}(\bar{y}) d\bar{y} = 0. \quad (23)$$

Substitution of Eq. (23) into Eq. (22) yields the thermal stress:

$$\left.\begin{aligned} \sigma_{xx}(\bar{y}) = \frac{E_i(\bar{y})}{1-\upsilon_i(\bar{y})} \times & \qquad (i = 1,2,3) \\ \left\{\frac{(B_2 D_0 - B_1 D_1) + (-B_1 D_0 + B_0 D_1)\bar{y}}{B_0 B_2 - B_1^2} - \alpha_i(\bar{y}) T'(\bar{y})\right\} & \end{aligned}\right\}, \quad (24)$$

where

$$\left.\begin{aligned} B_j &= \sum_i \int_{\bar{y}_{i-1}}^{\bar{y}_i} \frac{E_i(\bar{y})}{1-\upsilon_i(\bar{y})} \bar{y}^j d\bar{y}, \ j = 0,1,2 \\ D_j &= \sum_i \int_{\bar{y}_{i-1}}^{\bar{y}_i} \frac{\alpha_i(\bar{y}) E_i(\bar{y}) T'(\bar{y})}{1-\upsilon_i(\bar{y})} \bar{y}^j d\bar{y}, \ j = 0,1 \end{aligned}\right\}, \quad (25)$$

where B_j, D_j are calculated according to Simpson numerical integration method. It is necessary to illustrate that E, F and B denote elongation, free and bending, respectively. Such as EFBF denotes that the plate can elongate and bend freely.

V. Results and Discussion

A. Material Properties

To illustrate the foregoing analysis, numerical calculations have been carried out for a ZrO_2/FGM/Ti-6Al-4V composite plate. The constant properties of ceramics ZrO_2 and metal Ti-6Al-4V are shown in table 1[10].

© 2011 ACADEMY PUBLISHER

TABLE I.
MATERIAL PROPERTIES OF CERAMIC AND METAL

Properties \ Materials	ZrO_2	Ti-6Al-4V
Thermal conductivity rate, k / W (m K)$^{-1}$	2.09	7.50
Elastic modulus, E / GPa	151.0	116.7
Poisson's ratio, υ	1/3	1/3
Linear thermal expansion coefficient, α / K^{-1}	10.0×10^{-6}	9.5×10^{-6}

The volume fraction $V_m(\bar{y})$, $V_c(\bar{y})$ and porosity $P(\bar{y})$ in FGM gradient layer are shown as following [10-11]:

$$V_m(\bar{y})=\begin{cases}1-\bar{y}^M & M\geq 1\\ (1-\bar{y})^{1/M} & M<1\end{cases}, \quad (26)$$

$$V_c(\bar{y})=1-V_m(\bar{y}), \quad (27)$$

$$P(\bar{y})=A\bar{y}(1-\bar{y}),\quad 4>A\geq 0, \quad (28)$$

where M is the parameter of the material composition, A is the coefficient of porosity P. The volume fraction V_m ($\bar{y}$) under different M values is shown in Fig.2.

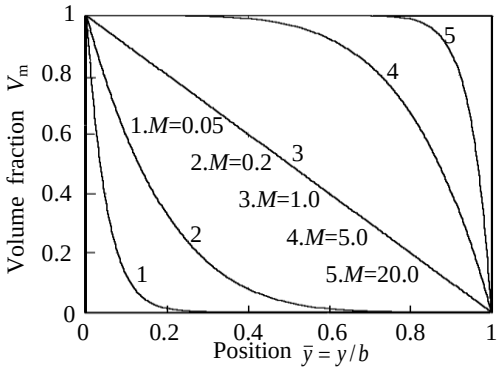

Figure 2. The volume fraction $V_m(\bar{y})$ of metal phase.

The material properties of the FGM gradient layer are given in the following form [10]:

$$k(\bar{y})=[(1-P^{1/3})/k_0+P^{1/3}/\{(1-P^{2/3})k_0+P^{2/3}k_a\}]^{-1}, \quad (29)$$

$$\left.\begin{aligned}E(\bar{y})&=E_0(1-P)/[1+P(5+8\upsilon_0)(37-\\ &\quad 8\upsilon_0)/\{8(1+\upsilon_0)(23+8\upsilon_0)\}]\\ \alpha(\bar{y})&=\alpha_0,\upsilon(\bar{y})=\upsilon_0\end{aligned}\right\}, \quad (30)$$

where $k(\bar{y})$, $E(\bar{y})$, $\alpha(\bar{y})$ and $\upsilon(\bar{y})$ and denote thermal conductivity, elastic modulus, thermal expansion coefficient and Poisson's ratio of the FGM gradient layer, respectively. Subscript a means air, and

$$k_0=k_c+3k_c(k_m-k_c)V_m(\bar{y})/\{3k_c+(k_m-k_c)V_c(\bar{y})\}, \quad (31)$$

$$\left.\begin{aligned}E_0&=E_c\{E_c+(E_m-E_c)V_m^{2/3}\}/\\ &\quad \{E_c+(E_m-E_c)(V_m^{2/3}-V_m)\}\\ \alpha_0&=[\alpha_mV_mE_m/(1-\upsilon_m)+\alpha_cV_cE_c/(1-\upsilon_c)]/\\ &\quad [V_mE_m/(1-\upsilon_m)+V_cE_c/(1-\upsilon_c)]\\ \upsilon_0&=\upsilon_mV_m+\upsilon_cV_c\end{aligned}\right\}, \quad (32)$$

where k_0, E_0, α_0 and υ_0 denote thermal conductivity, elastic modulus, thermal expansion coefficient and Poisson's ratio determined from the mixture rule, respectively.

B. Basic Parameters

The plate thickness b is 10 mm, and $h_1 = h_3$ in this paper. The finite element mesh of the ceramic/metal composite plate with FGM is divided into 1 280 elements and 1 282 nodes under convective heat transfer boundary condition, the smallest side length of the element is 0.015625 mm, T_0 = 300K.

C. Inspecting Validity of Method

The relative convective heat transfer coefficients on the lower and upper surfaces are denoted by $(\bar{\zeta}_a,\bar{\zeta}_b) = b \times(\zeta_a/k_m, \zeta_b/k_c)$. When $\bar{\zeta}_a=\bar{\zeta}_b=2000$, this corresponds to the fact that $\bar{\zeta}_a$ and $\bar{\zeta}_b$ tend to infinity, so we can introduce the first heating boundary condition.

Tables II and III show the inspecting results of heating steady temperature fields obtained from two different methods. From tables II and III, we know that the research method and numerical results in this paper are correct and reliable for the steady temperature fields.

TABLE II.

INSPECTING RESULTS OF HEATING STEADY TEMPERATURE FIELDS

	M=1, A=0		
$\bar{y}$	Analytical solutions[9]	FEM solutions	errors %
0.0	0.0000	0.0000	0.00
0.1	0.0531	0.0531	0.00
0.2	0.1135	0.1135	0.00
0.3	0.1821	0.1821	0.00
0.4	0.2598	0.2598	0.00
0.5	0.3478	0.3478	0.00
0.6	0.4473	0.4473	0.00
0.7	0.5601	0.5601	0.00
0.8	0.6880	0.6880	0.00
0.9	0.8336	0.8336	0.00
1.0	1.0000	1.0000	0.00

TABLE III.

INSPECTING RESULTS OF HEATING STEADY TEMPERATURE FIELDS

	M=1, A=2		
$\bar{y}$	Analytical solutions[9]	FEM solutions	errors %
0.0	0.0000	0.0000	0.00
0.1	0.0349	0.0349	0.00
0.2	0.0853	0.0852	0.12
0.3	0.1565	0.1563	0.13
0.4	0.2516	0.2514	0.08
0.5	0.3693	0.3690	0.08
0.6	0.5021	0.5019	0.04
0.7	0.6392	0.6391	0.02
0.8	0.7708	0.7707	0.01
0.9	0.8912	0.8912	0.00
1.0	1.0000	1.0000	0.00

Fig.3 shows the parameters and the heating steady thermal stress distribution that solved in this paper, and Fig.4 shows the parameters and the heating transient thermal stress distribution that solved in reference [10]. When the lower and upper surfaces are heated, compared

© 2011 ACADEMY PUBLISHER

with Fig.4, the steady thermal stress field distribution (t = 32 s) of Fig.3, as the whole, according to the method in this paper, we can know: the shape, bending degree, changing trend of the thermal stress curve and thermal stress value of corresponding points that obtained by the two methods are uniform apparently. So the research method and numerical results are correct and reliable for the steady thermal stress fields, and this proves the validity of the method in reference [10] at the same time.

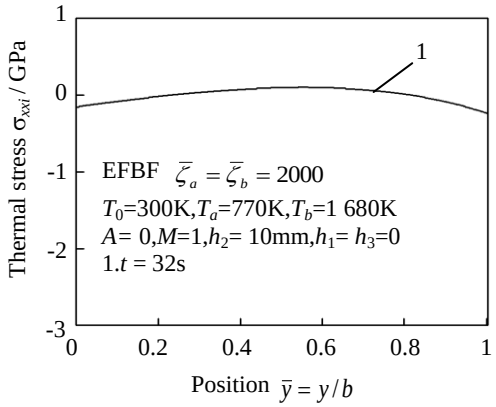

Figure 3. Steady thermal stress distribution in FGM plate.

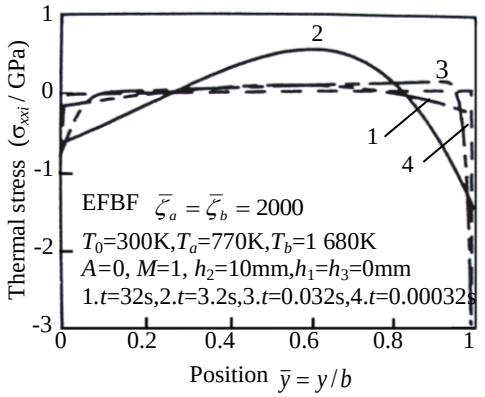

Figure 4. Transient thermal stress distribution in FGM plate.

D. Effect of FGM Layer Thickness

Fig. 5 shows the effect of the FGM layer thickness on temperature. We can know from Fig. 5 that the total change trend of the temperature in the composite plate is that the temperatures change from the smaller temperature in the metal layer to the larger temperature in the ceramic layer. In the metal and ceramic layers, the temperature figures are almost incline straight lines. The gradient of temperature curves in the metal layer is smaller than that of temperature curves in the ceramic layer obviously. But in the FGM layer, the temperature figure is curve, with the increase of the FGM layer thickness, the temperature curves tend to gentle and the temperature distribution in the composite plate is more reasonable. It is noteworthy that the maximum temperature value in the metal surface is 524.2 K and the maximum temperature value in the ceramic surface is 1 012K. Above regular phenomenon is induced by adopting convective heat transfer boundary condition.

Fig. 6 shows the effect of the FGM layer thickness on thermal stress. We can know from Fig. 6, in the metal and ceramic layers, the thermal stress figures are almost incline straight lines and the slope of each curve is slightly different. But in the FGM layer, the thermal stress figure is curve and the thermal tensile stress reaches the largest. The compressive stress on the metal surface reaches maximum when h_2=2mm. The compressive stress on the metal surface reaches minimum when h_2=6mm. In one word, with the increase of the FGM layer thickness, the thermal stress curves tend to gentle and the stress distribution in the composite plate is more reasonable, and the largest tensile stress of the EFBF composite plate reduces by 36.3%, and also the compressive stress on the metal surface reduces by 17.6%.

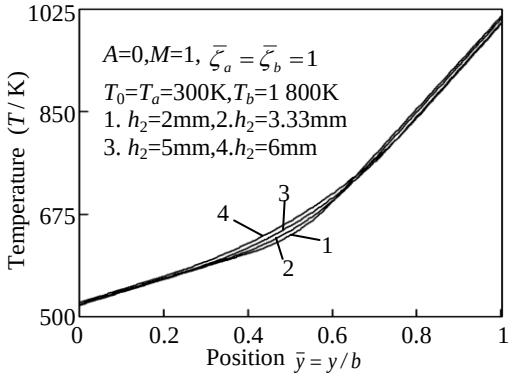

Figure 5. Effect of FGM layer thickness on temperature field.

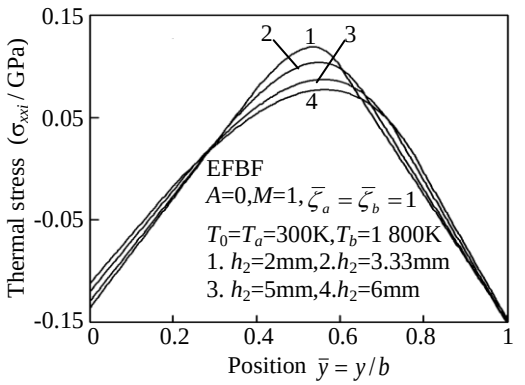

Figure 6. Effect of FGM layer thickness on thermal stress field.

E. Effect of FGM Layer Composition

Fig. 7 shows the effect of the FGM layer composition on temperature. We can know from the comparison in the curves of Fig.7 that when M=0.2 (curve 1) the temperature reaches the minimum on the metal surface, and the maximum on the surface of ceramics. Also, when M=1(curve 2), the temperature curve is comparative gentle and smooth, the temperature gradient is between curves 1 and 3, and the temperature distribution in the composite plate is more reasonable. When M=5 (curve 3) the temperature reaches the maximum on the metal surface, and the minimum on the surface of ceramics. In one word, with the increase of M, the temperature on the

© 2011 ACADEMY PUBLISHER

metal surface increases by 3.8%, and the temperature on the surface of ceramics reduces by 6.2%.

Fig. 8 shows the effect of the FGM layer composition on thermal stress. We can know from the comparison in the curves of Fig. 8 that when M=0.2 (curve 1) the compressive stress reaches the largest on the metal surface, and the minimum on the surface of ceramics. Also, when M=1(curve 2), the thermal stress curve is comparative gentle and smooth, the thermal stress gradient is between curves 1 and 3, and the stress distribution in the composite plate is more reasonable. When M=5 (curve 3) the compressive stress reaches the minimum on the metal surface, and the maximum on the surface of ceramics. In one word, with the increase of M, the compressive stress on the metal surface reduces by 28.3%, and the compressive stress on the surface of ceramics increases by 70.2%.

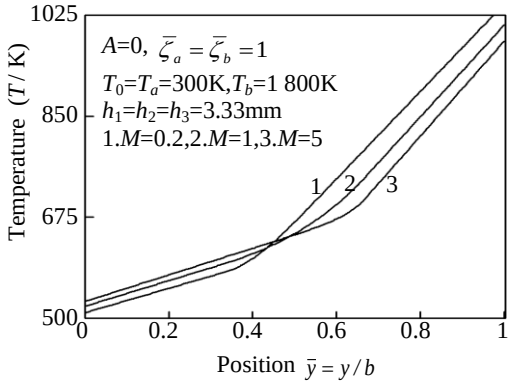

Figure 7. Effect of FGM layer composition on temperature field.

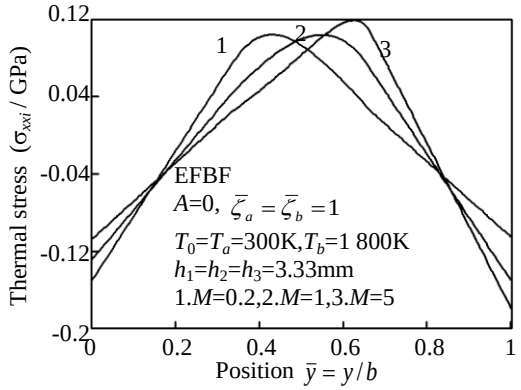

Figure 8. Effect of FGM layer composition on thermal stress field.

F. Effect of FGM Layer Porosity

We select the air thermal conductivity rate ka=0.02757 W/m K. Fig.9 shows the effect of the FGM layer porosity on temperature. When A=0 (curve 1), the temperature curve is gentle and smooth, and the temperature reaches the minimum on the surface of ceramics, its value is 521K, the maximum on the metal surface, its value is 1 007.6 K. When A=3.99 (curve 5), the variations of the temperature curve becomes big obviously, but the temperature curve is gentle and smooth at the bonding interfaces of the three-layered plate, and there is a abrupt change for temperature at the $\bar{y} \approx 0.48$, its value is 875 K, and the temperature reaches the maximum on the surface of ceramics, its value is 1 475.5 K, the minimum on the metal surface, its value is 380.7 K. It is noteworthy that compared with A=0, when A=3.99, the maximum temperature on the surface of ceramics increases by 46.4 %, and the maximum temperature on the surface of metal reduces by 26.9%.

Fig. 10 shows the effect of the FGM layer porosity on thermal stress. When A=0 (curve 1), the thermal stress curve is gentle and smooth, and the compressive stress reaches the maximum on the surface of ceramics, the minimum on the metal surface. When A=3.99 (curve 5), the variations of the thermal stress curve at the bonding interfaces of the three-layered plate becomes big obviously, and the curves appear sharp angle, and the maximum tensile stress value of curve 5 at the interface between metal layer and FGM layer is 9.76 times that of curve 1, and compressive stress on the metal surface increases by 61.9%. It is noteworthy that the tensile stress on the surface of ceramics reaches the maximum. Because it is weak in tension, so the large tensile stress is unfavorable to the strength of ceramics.

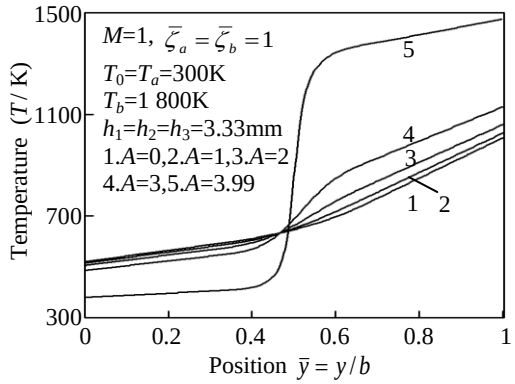

Figure 9. Effect of FGM layer porosity on temperature field.

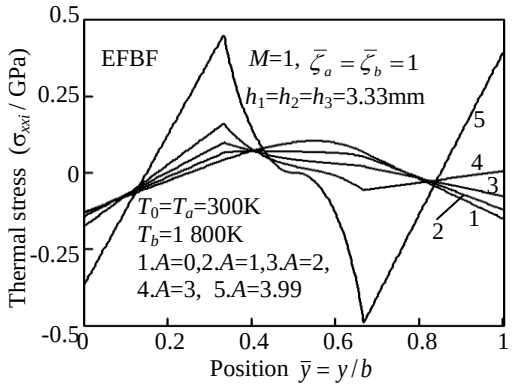

Figure 10. Effect of FGM layer porosity on thermal stress field.

G. Effect of Different Composite Plate

Fig. 11 shows the effect of the different composite plate on temperature. In the metal layer, the variation law of the temperature curves of two composite plate is similar, and the temperature figures are almost incline straight lines, and the gradient of temperature curves is almost same. But, in the ceramic layer, although the temperature figures of two composite plate are almost incline straight lines, the gradient of temperature curves is

© 2011 ACADEMY PUBLISHER

different, the gradient of temperature curve 1 in the nongraded two-layered composite plate is larger than that in the temperature curve 2 of the ceramic/metal composite plate with an interlayer of FGM. It is noteworthy that the temperature variation at the bonding interface in the nongraded two-layered composite plate becomes large, as shown in curve 1, and the curve appears obtuse angle. Compared with curve 2, the curve 1 of the ceramic/metal composite plate with an interlayer of FGM is very gentle and smooth.

Fig.12 shows the effect of the different composite plate on thermal stress. In the ceramic and metal layers, the whole variation law of thermal stress curves 1 and 2 is similar, although the temperature figures of two composite plate are almost incline straight lines, the gradient of temperature curves is different. But the thermal stress variation at the bonding interface in the nongraded two-layered composite plate becomes large, as shown in curve 1, and the curve appears sharp angle and reaches peak value. Compared with curve 1, the thermal stress curve 2 of the ceramic/metal composite plate with an interlayer of FGM is very gentle and smooth, and the maximum tensile stress reduces by 49.2%.

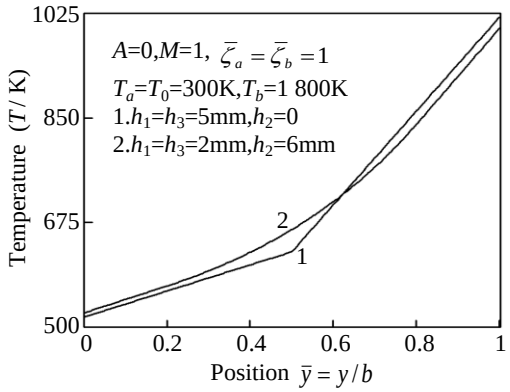

Figure 11. Effect of different composite plate on temperature field.

H. Effect of Convective Heat Transfer Coefficient

Fig. 13 shows the effect of the convective heat transfer coefficient on temperature. With the increase of the convective heat transfer coefficient, the variations of temperature curves become big, and the temperature curve 1 is more gentle and smooth than curve 2, and the slope of the curve 2 is bigger than that of curve 1 obviously. Compared with the curve 1, in the curve 2, the temperature on the surface of metal reduces by 23.9%, and the temperature on the surface of ceramics increases by 44.4%.

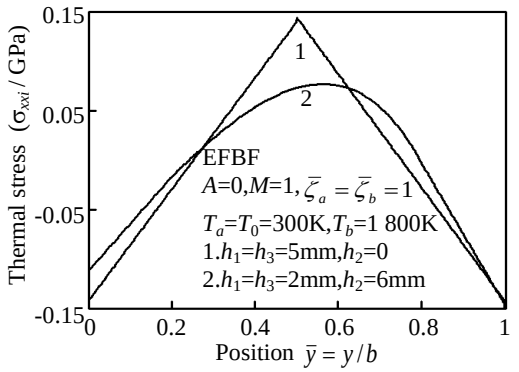

Figure 12. Effect of different composite plate on thermal stress field.

Fig. 14 shows the effect of the convective heat transfer coefficient on thermal stress. With the increase of the convective heat transfer coefficient, the variations of thermal stress curves become big, and the thermal stress curve 1 is more gentle and smooth than curve 2, and the slope of the curve 2 is bigger than that of curve 1 obviously. Compared with the curve 1, in the curve 2, the maximum compressive stress on the surface of metal increases by 148%, and the maximum tensile stress at the interface between FGM layer and ceramic layer increases by 61.8%, and the maximum compressive stress on the surface of ceramics increases by 165%.

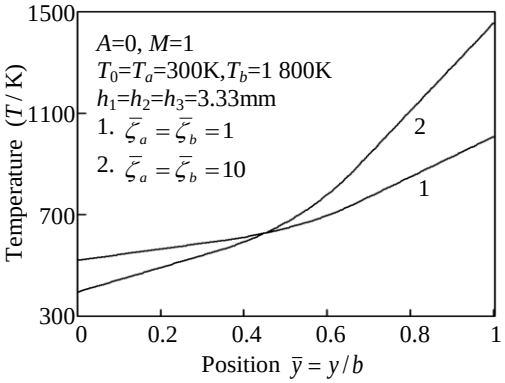

Figure 13. Effect of convective heat transfer coefficient on temperature field.

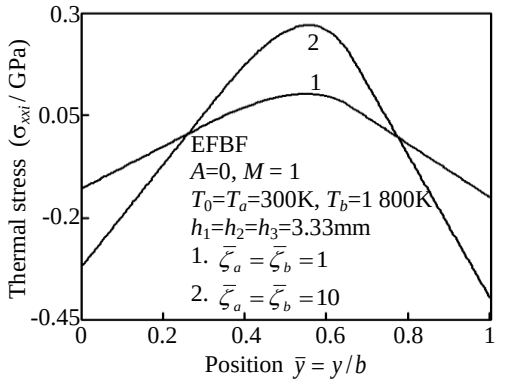

Figure 14. Effect of convective heat transfer coefficient on thermal stress field.

IV. CONCLUSIONS

We select a three-layered ceramic/metal composite EFBF in finite long plate with an interlayer of FGM as analytical model. The thermal boundary condition that we consider is convective heat transfer. According to thermoelasticity theory, we derive the finite element basic equation of the one-dimensional heat conduction of the composite plate by using of variational principle. We present a Sinpson method for the solution of steady thermal stress formulas of the composite plate. Using FORTRAN language we design the calculation software to obtain numerical results. From numerical calculation,

© 2011 ACADEMY PUBLISHER

when $\bar{\zeta}_a = \bar{\zeta}_b = 1$, T_0=T_a=300K and T_b=1 800K, the thermal stress distributions and the effect factors are discussed. The numerical results are as follows.

(1) With the increase of the FGM layer thickness, the temperature distribution in the composite plate is more reasonable and compared with h_2=2mm the tensile stress of h_2=6mm reduces by 36.3%.

(2) With the increase of *M*, the temperature on the surface of ceramics reduces by 6.2%, the compressive stress on the metal surface reduces by 28.3%, and the compressive stress on the surface of ceramics increases by 70.2%.

(3) With the increase of porosity, there is a abrupt change for temperature at the $\bar{y} \approx 0.48$, its value is 875 K, and the change of stress at the interface of the three-layered plate increases, and the tensile stress on the surface of ceramics reaches the maximum.

(4) Compared with $\bar{\zeta}_a = \bar{\zeta}_b = 1$, when $\bar{\zeta}_a = \bar{\zeta}_b = 10$, the temperature on the surface of metal reduces by 23.9% and the temperature on the surface of ceramics increases by 44.4%, and the stress on the metal surface increases by 148% and the stress on the ceramic surface increases by 165%.

(5) Compared with the nongraded two-layered composite plate, the temperature and the thermal stress of the ceramic/FGM/metal composite plate is very gentle and smooth..

ACKNOWLEDGMENT

This work is supported by the natural science found and education department found (2003136) of Hebei province and Handan city science and technology department fund (0821120081-2).

REFERENCES

[1] B. L. Wang, S. Y. Du and J. C. Han Y. "Thermomechanical coupling analysis advances of functionally graded material structure," Advances in Mechanics, CMES, Beijing, vol. 29, no.4, pp. 528-548, Nov. 1999.

[2] Y. Li, Z. M. Zhang, and S. Y. Ma, " Progress of the study on thermal of heating-resisting functionally gradient materials," Advances in Mechanics, CMES, Beijing, vol. 30, no.4, pp. 571-580, Dec. 2000.

[3] X. H. Zhu and Z. Y. Meng, "Current research status and prospect of functionally gradient materials," Journal of Functional Materials, Chongqin, vol. 29, no.2, pp. 121-127, June 1998.

[4] H. S. Shen, "Bending, buckling and vibration of functionally graded plates and shells," Advances in Mechanics, CMES, Beijing, vol. 34, no.1, pp. 53-60, Feb. 2004.

[5] J. Zhao, X. Ai, Y. Z. Li, and Y. H. Zhou. "Thermal shock resistance of functionally gradient solid cylinders," Materials Science and Engineering A, vol.418, no. 1-2, pp. 99-110. 2006.

[6] T. J. Liu, Y. S. Wang, C. Z. Zhang, "Axisymmetric frictionless contact of functionally graded materials," Arch Appl Mech, vol. 78: 267-282, 2008.

[7] W. Q. Chen, Z. G. Bian, and H. J. Ding, "Three-dimensional vibration analysis of fluid-filled orthotropic FGM cylindrical shells," International Journal of Mechanical Sciences, vol. 46, no.1, pp.159-171, 2004.

[8] Z. F. Shi, T. T. Zhang, and H. J. Xiang, "Exact solutions of heterogeneous elastic hollow cylinders," Composite Structures, vol. 79, no. 1, pp. 140-147, 2007.

[9] Y. Obata and N. Noda, "Unsteady thermal stresses in a functionally gradient material plate (Analysis of One-Dimensional Unsteady Heat Transfer Problem)", Trans. JSME, Series A, JSME, Tokyo, vol. 59, no.4, pp. 1090-1096, April 1993.

[10] Y. Obata and N. Noda, "Unsteady thermal stresses in a functionally gradient material plate (Influence of heating and cooling conditions on unsteady thermal stresses)," Trans. JSME, Series A, JSME, Tokyo, vol. 59, no.4, pp. 1097-1103, April 1993.

[11] Y. Tanigawa, T. Akai, R. Kawamura, and N. Oka, "Transient heat conduction and thermal stress problems of a nonhomogeneous plate with temperature-dependent material properties," J. Thermal stresses, Taylor & Francis Ltd, Philadelphia, vol.19, no.1, pp. 77-102, Jan. 1996.

[12] J. Huang and Y. B. Lü, "Thermal elastic limit analysis of layered plates of ceramic/metal functionally graded material, " J. Wuhan Univ. Technol. (Trans. Sci. & Engrg.), Wuhan Univ., Wuhan, vol. 17, no.6, pp. 754-757, Dec. 2003.

[13] Y. J. Xu, J. J. Zhang, and D. H. Tu, "Transient thermal stress analysis of functionally gradient material plate with temperature-dependent material properties under convective heat transfer boundary, " Journal of Mechanical Engineering, CMES, Beijing, vol. 41, no.7, pp. 198-204, July 2005.

[14] Y. J. Xu, D. H. Tu, and S. J. Ma, "Transient thermal stress of functionally gradient material plate with temperature-dependent material properties during heating and cooling process, "Journal of Mechanical Strength, CMES, Beijing, vol.27, no.4, pp. 510-517, Aug. 2005.

[15] H. G. Wang, Introduction of thermal elasticity, Tsinghua Univ. Press: Beijing, 1989, pp.170-172.

Xu Yangjian (1956-) received his solid mechanics Master degree from Tianjin University, China in 1997. He is/was a Professor (from 2004), Mater's tutor in solid mechanics, Hebei University of Engineering, Handan, China. His research areas are solid mechanics and the application of FEM and the thermomechanical behavior of new type of materials. He has published over 40 academic papers in magazines and international conferences in his research fields. His 16 papers have been abstracted by EI.

Tu Daihui (1956-) received her Bachelor degree and Master degree from Chengdu gqing University and Taiyuan University, respectively, China in 1982 and 2002. She is/was a Professor (2008-now) in Hebei University of Engineering. **S**he has published over 30 academic papers in her research fields.

Du Haiyang (1985-) received his engineering mechanics Bachelor degree from Hebei University of Engineering, Handan, China, in 2009. Since 2009, he has been working towards the the Master degree of structural engineering in Hebei University of Engineering. He has published 3 papers in magazines and international conferences in his research fields.

© 2011 ACADEMY PUBLISHER